Renewable Energy 269 (2026) 125813

Contents lists available at ScienceDirect

Renewable Energy

journal homepage: www.elsevier.com/locate/renene

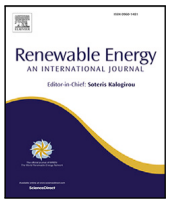

Assessing future climate change impacts on marine renewable energy resources in the UK under a high emission scenario with CMIP6 and SWAN

John-Luke McWhirter [a,*], Bahareh Kamranzad [a], George Lavidas [b], Gil Lemos [c]

[a] Department of Civil and Environmental Engineering , University of Strathclyde, James Weir Building, 75 Montrose Street, Glasgow, G1 1XJ, United Kingdom
[b] Marine Renewable Energies Lab, Offshore Engineering Section, Department of Hydraulic Engineering, Civil Engineering & Geosciences, Delft University of Technology, Stevinweg 1, Delft, 2628 CN, Netherlands
[c] Faculty of Sciences, University of Lisbon, Faculdade de Ciências, Instituto Dom Luiz, Lisbon, 1749-016, Portugal

ARTICLE INFO

Keywords:
Climate change
Wind energy
Wave energy
CMIP6
SWAN
UK

ABSTRACT

Marine resources such as wind and wave are expected to play an important role in decarbonising the UK's energy network, as part of the global transition from fossil fuels to renewable energy. However, potential increases in global weather systems variability due to climate change cast doubt on the long-term sustainability of offshore renewable development and the ambitions of the UK government to rapidly expand current capacity. As such, growing interest in co-located wind–wave systems is being paid as a means of enhancing the climate resilience of the future energy network. This study investigates the impacts of climate change on wind and wave resources in the UK from 2015 to 2100, using available CMIP6 datasets and numerical wave modelling using SWAN. In doing so, an initial assessment of the potential for co-located infrastructure is undertaken to inform future research into its role in strengthening the climate resilience of ocean renewable generation. The results reveal gradual reductions in resource availability under a high emission scenario, with statistically significant annual trends detected across most of the study area. Reductions in average annual wind energy reach −16.0% in coastal areas of Northern Ireland towards the end of the century, while decreases in wave energy of more than 25% are projected in certain regions of the North Sea. These trends are primarily driven by seasonal reductions during summer months, with decreases in average wind power during these months as much as −29.0% and decreases in wave power of over −40%. In addition, increases in resource variability from the mid-century onwards suggest that climate change is likely to negatively affect the availability of the UK's wind and wave energy resources in the long term.

1. Introduction

The 6th Assessment Report by the International Panel on Climate Change (IPCC) identifies greenhouse gas emissions as the leading driver of climate change, contributing to increasingly unstable global weather systems [1]. In addition to rising temperatures, climate change has been linked to the increasing occurrence and intensification of extreme weather events such as droughts, wildfires and storms, with direct consequences for people and ecosystems worldwide [2]. Energy production is estimated to account for approximately 76% of global emissions each year, placing the transition from fossil fuels to renewable energy sources at the centre of global climate change mitigation [3].

The potential role of marine resources in this transition, namely wind and wave energy, presents significant benefits over onshore alternatives. For offshore wind, this includes higher energy yields and reduced environmental impacts compared to onshore wind [4], while wave energy has been shown to provide more stable energy yields throughout the year than wind and solar [5]. Wave energy also presents strong logistical advantages for the access to clean power, given that two thirds of the world's population reside less than 60 km from coastal areas [6].

Since the 1980s, Europe has cultivated a leading role in the global energy transition, in large part through the rapid expansion of offshore wind projects [4]. At present, the UK is the region's leading developer of offshore wind, with the ambitious goal of quadrupling current capacity by 2030 [7]. This is parallel to growing interest in wave energy in both public and private sectors, including the recent establishment of the Marine Energy Taskforce in 2025, supported by the Crown Estate, to support the research and deployment of wave energy projects [8].

However, the integration of renewable energy at this rate and scale presents a number of significant challenges. From a supply perspective, renewable resources cannot be dispatched at need, causing problems

* Corresponding author.
E-mail address: j.mcwhirter@strath.ac.uk (J.-L. McWhirter).

https://doi.org/10.1016/j.renene.2026.125813
Received 16 January 2026; Received in revised form 16 April 2026; Accepted 16 April 2026
Available online 27 April 2026

for network operators who must balance supply and demand [9]. Moreover, energy systems with high levels of renewable penetration become overtly reliant on climate, rendering infrastructure vulnerable both to short term intermittency as well as large scale climatological impacts, such as climate change [10].

Diversification of renewable supply is considered one of the strongest methods to mitigate these impacts. This can be achieved through the co-location of different technologies to harness multiple types of resource at the same time and place. In an offshore context, benefits of combining wind and wave resources can include higher annual energy yields as well as reduced intermittences compared to individual resources [11]. The operational benefits of co-located wind and wave also include increased site accessibility as a result of shadowing effects, whereby an array of wave energy converters (WECs) can serve to absorb incoming wave energy during harsh weather conditions [12]. Previous research has indicated that European regions of the Atlantic Ocean are particularly promising for co-located wind-wave projects [13]. Meanwhile, increasing interest in hybrid projects is being paid in the UK by stakeholders in both public and private sectors [14]. The UK therefore presents a unique context within which to explore research opportunities for hybrid offshore infrastructure.

The potential for commercial scale integration of wave energy systems alongside existing offshore wind first warrants an investigation of long term climate impacts on respective wind and wave resources in the region. At present, joint energy assessments of wind-wave resources are important to understand resource dynamics and synergies but are largely dominated by the study of historical resource availability: [15] provides a regional assessment of offshore wind and wave resources across Europe using hindcast data for 2001–2010 and identified western offshore areas in the region as optimal for combined wind-wave systems based on theoretical resource availability. [16] performs a similar analysis in the Mediterranean Sea based on linear temporal correlations between wind-wave resources, based on WAVEWATCH3 simulations forced with reanalysis wind inputs. At a national scale, [17] analyses historical resource availability using ERA5 wind data to force a SWAN model for the coast of Portugal. [18] generates wave outputs using a WAVEWATCH3 model for Ireland, with input winds from the high-resolution HERMOINE dataset for the period 2000–2013. [19] adopts a spatial planning approach to assess correlations between wind speeds and significant wave heights across the Italian Peninsula, and contextualise results in relation to designated ecological reserves and industry infrastructure. Elsewhere, [20] conducts a local joint energy assessment for a proposed co-located wind-wave farm off the coast of Denmark.

On the other hand, assessments of future climate change impacts on renewable energy availability have primarily focused on standalone resources. For instance, [21] investigates future impacts on wind resources across northwestern Europe under two pathways using CMIP6 datasets, showing decreases in wind energy availability across the UK for both intermediate and high emission scenarios. [22] provides a similar assessment specifically for offshore areas, finding larger reductions in long term wind energy potentials under a high emission scenario. Wave energy has been similarly assessed separately for the region: [23] uses CMIP5 projection data to drive a nested wave model with WAVEWATCH3 and SWAN, and find decreases in wave energy potential across the northwestern Iberian Peninsula under a high emission scenario. [24] assesses future impacts on the economic viability of wave energy and evaluate the performance of fourteen WEC technologies, with a focus on profitability measured in terms of the Levelised Cost of Energy (LCOE).

In comparison, joint assessments of wind-wave resources for future periods across Europe remain limited. An exception is found in [25], where an assessment of solar, wind and wave resources is conducted using CMIP6 data under a high emission scenario for areas of the Atlantic coast and the Mediterranean basin. In doing so, decreases in wave energy are detected for the remainder of the 21st century, while synergies between resources remain relatively unchanged. However, within this unique subfield, a comprehensive national-scale assessment quantifying the future impacts of climate change on the UK's wind-wave resources based on the latest generation of global climate models is currently lacking.

The novelty of this study is to utilise multiple Coupled Model Intercomparison Project phase 6 (CMIP6) datasets to assess climate change impacts on these marine resources within the UK's Exclusive Economic Zone (EEZ) and serves as an initial assessment to improve understanding of the long-term potential for co-located wind–wave systems. This is achieved through an investigation of spatiotemporal trends in theoretical resource availability for multiple future periods (2025–2049, 2050–2074 and 2075–2099), relative to a present-day baseline (2015–2024), as well as continuous resource evolutions over time. In doing so, the research novelty is twofold: firstly, a multi-model wind and wave energy ensemble is created specific to the UK EEZ for a high emission scenario (SSP5-8.5), with direct relevance for policy makers and industry stakeholders. Applying the same methodological framework to both wind and wave resources addresses methodological inconsistency between previous studies of standalone resources, and allows resource changes to be quantified on a comparable basis. Secondly, this study provides a robust assessment of future impacts on wind and wave resources in the UK under a worst case climate change scenario, with implications for future renewable development. This is primarily achieved through the use of a Multi-Model Ensemble (MME) approach, comprised of datasets of high temporal resolution (three hourly), allowing to minimise errors resulting from single model bias, to better depict uncertainty, and deliver more reliable long term climate signals.

The structure of the present study is as follows: Section 2 provides an overview of the data used and the applied methodology. Section 3 will present and discuss key research findings, with references to external research findings, followed by a summary of conclusions and underlying limitations in Section 4.

2. Materials & methods

2.0.1. The 6th coupled model intercomparison project (CMIP6)

Climate projection datasets provide valuable information on future climate systems for a range of variables, including those relevant to renewable energy production. The most frequently utilised group of these models within contemporary energy assessment literature are those developed under the Coupled Intercomparison Project (CMIP), coordinated by the World Climate Research Program (WCRP). The 6th phase of CMIP (CMIP6) is the most recent publicly available iteration, with climatological institutions around the world contributing with single models using several controls, the most important being the presence of anthropological greenhouse gas emissions in the Earth's atmosphere. CMIP6 data are available for a number of Shared Socioeconomic Pathways (SSPs), each representing a potential future climate change outcome, which accounts for variations in collective societal responses to climate change, including adaptation and mitigation, as well as the amount of greenhouse gas emissions, reflected by a radiative forcing level [1]. Of these, SSP5-8.5 represents a future dominated by fossil fuel development, characterised by rapid global economic growth coupled with continued reliance on fossil fuel resources and increasing global energy demands [26]. This scenario is among the most frequently researched in resource assessment literature as the worst case scenario for climate change, and is not often considered in future planning for sustainable development of marine renewables.

Data for eight CMIP6 datasets were obtained with global coverage from the Earth System Grid Federation (ESGF) nodes, based on the availability of three hourly average vertical and horizontal near surface (10 m) wind speed variables, with full coverage from 2015 to 2100 (Table 1). This was determined the minimal temporal resolution required to force a numerical wave model, and datasets were selected based on their availability at these intervals. All were obtained under the same variant label (r1i1p1f1) to ensure consistency across ensemble members (r1), initialisation method (i1), physics (p1), and forcing (f1).

Table 1
Available CMIP6 datasets and their spatial resolutions.

Model	Longitude resolution	Latitude resolution
CMCC-CM2-SR5	1.25°	0.94°
CMCC-ESM2	1.25°	0.94°
IPSL-CM6A-LR	2.50°	1.27°
MPI-ESM1-2-LR	1.88°	1.86°
EC-Earth3	0.70°	0.70°
EC-Earth3-Veg	0.70°	0.70°
MIROC6	1.41°	1.40°
GFDL-ESM4	1.25°	1.00°

Table 2
Wave buoy identifiers and spatial properties. Proximity to shore relates to the nearest distance to the UK mainland.

Alias	Longitude	Latitude	Depth (m)	Proximity to Shore (km)
Tyne/Tees	−0.786°	54.9189°	63	67
Hastings	0.7547°	50.7461°	37	15
SW Isles of Scilly	−6.5444°	49.8167°	91	101
Blackstones	7.0567°	56.0619°	96	77
Moray Firth	−3.3331°	57.9664°	50	45

2.0.2. ECMWF reanalysis version 5 (ERA5)

Reanalysis datasets seek to assimilate historical observations into numerical climate models, using data from meteorological stations, wave buoys and satellites, to create highly accurate estimations of past climate. The latest version of the European Centre for Medium Range Weather Forecasts (ECMWF) Reanalysis dataset (ERA5) provides high resolution climate data from 1940 to present at hourly intervals, and is widely utilised across energy assessment literature, both to evaluate hindcast data and to assess resources.

ERA5 has been shown to perform more accurately than alternative reanalysis datasets such as MERRA2 for key variables including wind speed [27] and solar irradiance [10]. Moreover, numerical wave models forced using ERA5 wind data have demonstrated better accuracy than others such as CFSv2, important for the successful calibration of the wave model [28]. Limitations of using ERA5 to drive numerical wave models have been shown to include underestimations in wave power, particularly for swell-exposed locations [29], necessitating comprehensive model calibration targetting swell dissipation and windscaling (see Section 2.1.2).

For the purposes of evaluating the CMIP6 datasets and to calibrate the numerical wave model, three hourly averages were derived from hourly ERA5 data for vertical and horizontal near surface wind speeds, obtained from the Copernicus Climate Data Store, at a spatial resolution of 0.25° for northwestern Europe (−30 W to 25 E and 35 N to 75 N) for 2015 to 2024.

Bathymetry data was obtained from the General Bathymetric Chart of the Oceans (GEBCO) at a spatial resolution of 0.0042°. Data was obtained for the area −22.5 W to 5.5 E and 39 N to 70 N, to encompass the full extent of the study area including the computational grid of the parent wave model (Fig. 1).

To calibrate and validate wave model outputs, in-situ wave data was obtained from the *WaveNet* data portal, run by the Centre for Environment, Fisheries and Aquaculture Science (CEFAS), for five wave buoys located around the UK coastline (Table 2, Fig. 2). Post-recovery data for significant wave height (H_s) and average zero crossing period (T_z) were acquired for 2015 to 2024 at 30 min intervals. The data undergoes a number of quality control procedures as it is collected, where recorded values are screened to remove invalid entries based on set maximum rates of change per hour [30]. Thus, raw observed values were determined to be of sufficient quality for the purposes of calibrating the numerical wave model.

Several datasets were sourced to define the study area using administrative boundaries. Maritime limits were obtained from the UK Hydrographic Office, which provides data for the UK's EEZ, as well as the Scottish Government's marine open data network, which provides data for Scottish Marine Regions. Within the EEZ, water depths reach 4354 m, with the deepest waters located in the north along the European continental shelf, which greatly exceeds the maximum depth for floating wind projects and commercial scale wave energy converters (WECs) [31].

In order to maximise the relevancy of findings, the study area was modified to exclude a number of Scottish Marine Regions, namely Rockall, the Faroe Shetland Channel and Bailey, where mean water depths exceed 1300 m (Fig. 2). The following analysis therefore concerns administrative areas of the EEZ wherein commercial scale co-located wind-wave projects can potentially be feasible in the future.

2.1. Methodology

All eight CMIP6 datasets and the ERA5 dataset were re-gridded to 0.5° to using the first order conservative method, to enable cross comparison whilst preserving minimum and maximum values [32]. The magnitude of wind speed at 10 m (U_{10}) was then derived from horizontal (u) and vertical (v) components as:

$$U_{10} = \sqrt{u^2 + v^2} \tag{1}$$

In the absence of technical specifications for any single turbine design, theoretical wind energy can be calculated as the Wind Power Density (WPD), a product of the cube of wind speed:

$$WPD = 0.5\rho_a U_{100}^3 \tag{2}$$

Where ρ_a is the air density (1.225 kgm^{-3}) and U_{100} is the wind speed magnitude at 100 m height, a typical hub height for offshore wind turbines, which can be extrapolated using Power Law as:

$$U_{100} = U_{10}\left(\frac{Z}{Z_r}\right)^{\alpha} \tag{3}$$

Where Z_r is the height of near surface wind speed (10 m) and α is the wind shear exponent. Because the analysis concerns coastal and offshore resource only, a constant α value of 0.11 was used to represent the rate at which wind speed increases with height for sea surface areas [33].

To quantify theoretical wave energy, Wave Energy Flux (WEF) can be used as a function of significant wave height (H_s) and absolute energy period (T_a) as:

$$WEF = \frac{\rho_o g^2}{64\pi} H_s^2 T_a \tag{4}$$

Where ρ_o is the ocean water density (1025 kgm^{-3}) and g denotes gravitational acceleration (9.81 ms^{-2}).

2.1.1. CMIP6 dataset evaluation

The deployment of climate projection data for the assessment of resource potential warrants an investigation of how well each dataset simulates wind climate. To understand the geographical variance in model accuracy, the relative bias at each grid point was quantified with respect to monthly average near surface wind speed magnitude values by calculating the mean absolute percentage error (MAPE, Eq. (5)), as well as the corresponding magnitude of error as the mean absolute error (MAE, Eq. (6)):

$$MAPE = 100 \times \frac{1}{N}\sum \frac{|x_i - y_i|}{x_i} \tag{5}$$

$$MAE = \frac{1}{N}\sum |x_i - y_i| \tag{6}$$

Where N is the total number of paired values, while x_i and y_i represent the observed and modelled values, respectively. Each atmospheric model is evaluated based on the magnitude of error at each grid cell, where MAPE values exceeding 100% are considered unreliable for

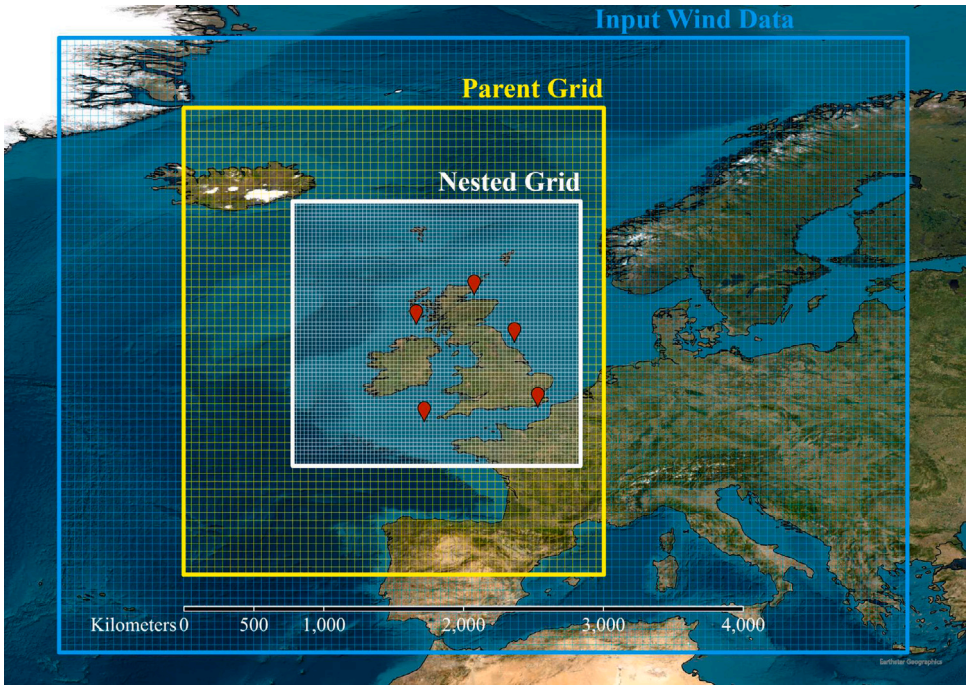

Fig. 1. Computational grids used for the SWAN model in relation to the wave buoy locations (shown in red) used for model calibration.

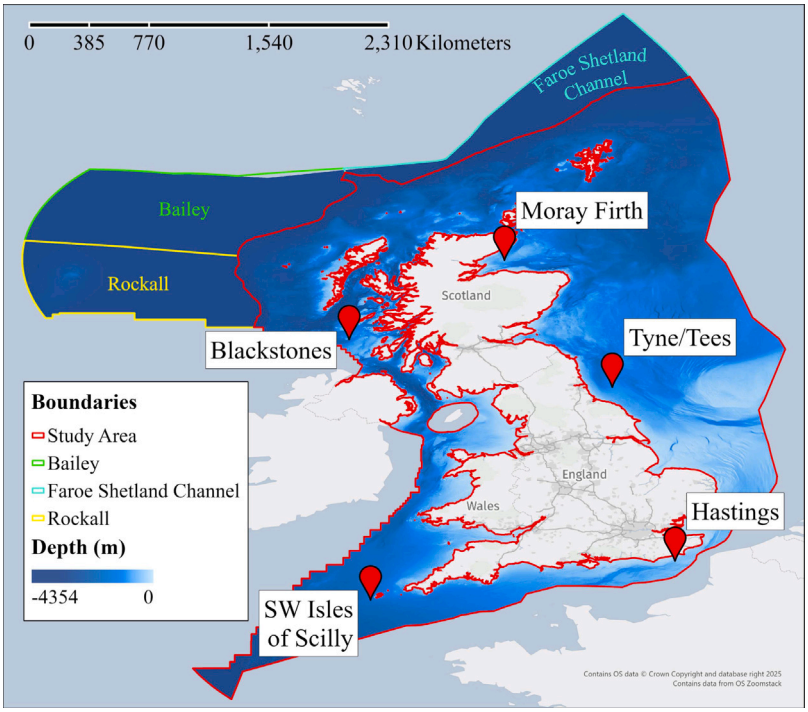

Fig. 2. Wave buoy locations and bathymetry across the study area. Highlighted areas indicate Scottish Marine Regions excluded from the study due to high mean water depths exceeding 1300 m. As a Crown Dependency, the Isle of Man is not part of the UK's EEZ.

drawing statistical conclusions. Therefore, any dataset in which more than 10% of grid points exceed this threshold will be excluded from the analysis to safeguard the quality of subsequently derived resource potentials. These criteria were informed from an examination of the spatial distribution of MAPE values across datasets, which indicated that the chosen threshold effectively distinguished datasets exhibiting disproportionately large errors.

2.1.2. *Numerical wave modelling*

Simulating WAves Nearshore (SWAN) is third generation spectral wave model developed by *Delft University of Technology* and is primarily intended for coastal applications and nearshore environments, with implicit non-linear solutions for terms such as depth breaking, triads, etc. It applies the action balance equation (Eq. (7)) to generate wave characteristics using a series of inputs, including near surface wind

Table 3
Validation periods assigned to each buoy.

Alias	Start date	End date
Tyne/Tees	2015-01-01	2015-03-14
Hastings	2017-03-15	2017-05-26
SW Isles of Scilly	2019-05-27	2019-08-07
Blackstones	2021-08-08	2021-10-19
Moray Firth	2023-10-20	2023-12-31

speed and bathymetry:

$$\frac{\partial N}{\partial t} + \frac{\partial}{\partial x}\left(c_x N\right) + \frac{\partial}{\partial y}\left(c_y N\right) + \frac{\partial}{\partial \sigma}\left(c_\sigma N\right) + \frac{\partial}{\partial \theta}\left(c_\theta N\right) = \frac{S}{\sigma} \tag{7}$$

Where N is the action density function of intrinsic frequency (σ), wave direction (θ), spatial coordinates (x, y), and time (t). The first term describes the temporal variation of N, followed by terms representing its propagation in geographical space (x, y), frequency space (σ), and directional space (θ), with c_x, c_y, c_σ, and c_θ denoting the corresponding propagation velocities. The source term S accounts for energy generation by wind, dissipation (through white-capping, depth-induced breaking, and bottom friction), and nonlinear wave–wave interactions [34].

Since its inception, SWAN has been deployed extensively across engineering disciplines to simulate offshore wave climate [35]. Within energy assessment literature, this has mostly been applied to assess resources for historical periods [36] but has also been used to determine future climate using projection data [25]. In the present study, a nested SWAN model for a regular grid was carried out to simulate the ocean environment with boundary conditions (Fig. 1). These were calculated for a 0.5° grid, while nested outputs were calculated at 0.25°, both at computational intervals of 30 min.

To determine optimal physics for simulating real wave climate, the model was forced using the near surface directional wind speed components of the remapped ERA5 wind data and calibrated for the year 2015 against observed wave buoy data for individual variables H_s and T_z. Although ERA5 is available at finer resolution, the model was calibrated and validated using the coarse spatiotemporal grid to more accurately reflect performance at similar resolution and to avoid interpolation biases.

Upon optimisation of model physics, 30 min output values for each variable were then generated for the full baseline period before being used to derive WEF as a product of H_s and T_z, in the absence of observed values for T_a. Results for WEF, as well as H_s and T_z, were then validated by allocating each point a unique window of 73 days in the baseline period (one fifth of a 365 day year), in order to provide a balanced and comprehensive assessment of model accuracy for each location (Table 3). Throughout the calibration and validation phases, the performance of the wave model was assessed using a number of metrics to determine the bias (Eq. (8)), root mean squared error (RMSE, Eq. (9)), and scatter index (SI, Eq. (10)) and correlation (CC, Eq. (11)) relative to observed values:

$$bias = \bar{y} - \bar{x} \tag{8}$$

$$RMSE = \sqrt{\frac{1}{N}\sum (y_i - x_i)^2} \tag{9}$$

$$SI = \frac{RMSE}{\bar{x}} \tag{10}$$

$$CC = \frac{\sum (y_i - \bar{y})(x_i - \bar{x})}{\sqrt{\sum (y_i - \bar{y})^2}\sqrt{\sum (x_i - \bar{x})^2}} \tag{11}$$

Where x_i is the observed value at interval i, y_i is the model output and $\bar{x}$ and $\bar{y}$ represent the mean of observed and modelled values, respectively. Upon validation of the results, the model was forced using the directional near surface wind components of each CMIP6 dataset. Due to computational resource constraints, outputs were generated at three hourly intervals.

2.1.3. Multi-Model Ensembles (MMEs)

Due to the non-linearity of both WPD and WEF, two Multi-Model Ensembles (MMEs) were derived as a simple average of daily mean WPD and WEF values, respectively. This procedure was applied across the CMIP6 datasets deemed of sufficient quality from the results of the evaluation. Combining models in this way helps reduce single model biases, based on the assumption that errors will cancel out; also providing a better representation of the associated uncertainty, in line with the number of models included [37]. This approach is commonplace in energy assessments for future periods that utilise multiple single models, and presents an alternative to the application of bias correction to individual datasets [22].

However, MMEs constructed for individual variables prior to the computation of final variables have been shown to severely underestimate wave power [38]. Tests conducted within this study confirmed this, whilst showing underestimations in modelled WPD according to an average of raw near surface wind speeds. Additionally, the sequence of resource calculation was shown to impact the strength of climate impact over time, as MMEs of raw variables elicited weaker climate signals than those constructed from modelled resources of single models. Thus, resources were assessed using MMEs, as the average of single model wind and wave resources, respectively.

To assess implementation of the MME method, hindcast data for the baseline period was evaluated against ERA5 using a number of statistical measures applied to the monthly resampled data series of WPD values, for single CMIP6 datasets as well as the wind MME, within the study area. Namely, the correlation coefficient (CC, Eq. (11)), standard deviation (σ, Eq. (12)) of each model, as well as the centred root mean squared difference (CRMSD, Eq. (13)) relative to ERA5 values:

$$\sigma = \frac{1}{N}\sqrt{\sum |y_i - \bar{y}|^2} \tag{12}$$

$$CRMSD = \frac{1}{N}\sqrt{\sum \left[\left(y_i - \bar{y}\right) - \left(x_i - \bar{x}\right)\right]^2} \tag{13}$$

To properly quantify climate impacts, analyses must be conducted at broad temporal horizons spanning multi-decadal periods relative to a historical baseline. Therefore, each MME was divided into four different time periods to define the present-day baseline (2015–2024), near future (2025–2049), mid future (2050–2074) and far future (2075–2099) periods to fully account for the remainder of the 21st century.

In addition, to comparing multi-decadal periods, the strength and significance of continuous change over time was conducted by applying a linear regression to each grid point. This was applied to each MME after removal of seasonal bias, whereby monthly average values were subtracted from the full 85 year study period, in order to elicit a clearer climate signal. The temporal variability of renewable resources has significant implications for project development, where more stable resource output is more desirable from both investor and grid control standpoints. The stability of each resource was therefore measured by applying the Coefficient of Variation (CoV, Eq. (14)) to daily average values of each MME, to understand the variability of resources relative to the mean of each period:

$$CoV = \frac{\sigma}{\bar{x}} \tag{14}$$

3. Results & discussion

3.1. Evaluation of CMIP6 datasets

Grid-point evaluation of single-model bias shows pronounced geographic variation in each dataset's accuracy in representing past near-surface wind speed magnitudes.(Fig. 3). It can be observed that the models generally perform better for offshore areas than onshore and coastal regions. This is attributable to poorer quality altimeter data for coastal areas [39], which is typically used to calibrate atmospheric

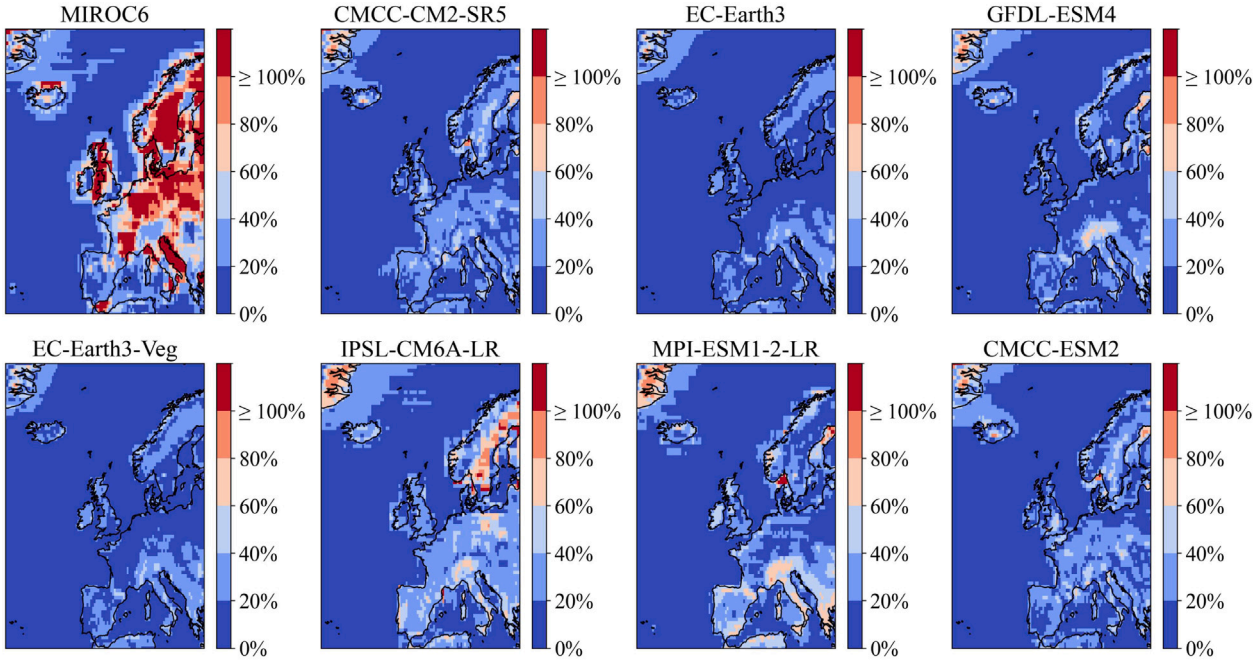

Fig. 3. MAPE values for monthly average near surface wind speed magnitudes across all single CMIP6 datasets.

models, as well as oversimplification of onshore topography due to the coarse spatial resolution of the data [40].

Of all eight CMIP6 datasets, the EC-Earth3-Veg and EC-Earth3 datasets demonstrate the lowest grid averaged MAPE values of 17.1% and 17.2%, respectively, both with grid averaged MAE values of 1.04 ms^{-1}. This is consistent with previous studies, which also identify the EC-Earth3 model as one of the best-performing CMIP6 datasets for wind speeds over northwestern Europe based on its distributional similarity to ERA5 [21]. MIROC6 shows the weakest performance, characterised by higher MAE values, particularly over mainland Europe, with a high grid averaged MAPE of 44.4%. These disparities are even more pronounced within the study area, wherein MIROC6 displays a grid average MAPE of 53.5%, with 15.6% of grid points with MAPE values over 100%. In comparison, MAPE values do not exceed 85.4% at any given grid point within the study area for the remaining datasets. Thus, the decision was made to exclude MIROC6 from both wind and wave MMEs to safeguard the quality of research findings.

To compare the overall performances of the selected CMIP6 datasets and the resultant wind MME, statistical properties for monthly average WPD values within the study area were plotted using a Taylor diagram (Fig. 4). Here, datasets at finer spatial resolutions are shown to outperform those at coarser scales, while the MME results in an increased correlation with ERA5 (0.83), as well as a reduction in CRMSE to 0.44 kWm^{-2}. The MME of WPD is thus shown to effectively reduce single model bias while more accurately representing wind resources within the study area for the baseline period.

3.2. Wave model performance

The calibration of the wave model concluded the Source Term 6 (ST6) wave growth package as the optimal choice based on the results compared for all five buoy locations. Unlike alternative parameterisation schemes such as KOMEN and WESTH, wave dissipation under ST6 comprises two terms to account for local and cumulative dissipation independently [41]. This defines how the wave model accounts for the rate of energy dissipation that occurs due to wind-wave interaction at the sea surface. ST6 also enables model calibration for a wider range of physical properties such as dissipation due to swell and windscaling.

Through an iterative process, combinations for local and cumulative dissipation terms and their associated power coefficients, using calibrated values listed in the SWAN user manual, and empirical values from [41], were tested against various windscaling values. Further experimentation found that wind drag according to [42] simulated more realistic wave outputs according to observed data, in line with findings from calibration studies that used ERA5 wind data with ST6 parameterisation [43]. Other key parameters that were adjusted to improve model performance included dissipation due to bottom friction, swell dissipation, and numerical procedures for non-linear computation of quadruplet wave interactions. More information on calibrating SWAN for ST6 can be found in [41,43].

Table 4 shows the results of the model validation for each variable for the buoy locations. As shown, the model performs strongly for H_s, with a bias ranging from −0.16 m at Blackstones to 0.10 m at Tyne/Tees, with an average absolute error of 0.09 m. In terms of wave power, the biases for the above mentioned locations are −3.73 kWm^{-1} and 0.71 kWm^{-1}, respectively, with an average absolute error of 1.25 kWm^{-1}. Meanwhile, T_z is generally underestimated across all locations with higher RMSE and lower correlations, although with reasonable values for SI as low as 0.17. This is reflected in the wave power product of T_z, which is shown to underestimate wave energy yields at three of the five locations. However, correlation for wave power ranges between 0.82 at Blackstones and 0.97 at Tyne/Tees, indicating strong model performance for energy capture.

The propagation of residual errors in the wave model over time are shown in Fig. 5, with implications for long term statistical results. Despite positive bias detected at Moray Firth during validation, the model slightly underestimates average annual WEF for the baseline period by −5.6%. On the other hand, the sizeable negative bias at Blackstones propagates an underestimation of −22.4% for average annual WEF, rendering absolute changes over time in these areas less reliable than regions dominated by locally generated wind-waves. However, the high level of correlation between observed and modelled values at Blackstones suggests that relative changes are still well captured by the model if it is assumed residual uncertainty introduced by the wave model remains constant between the baseline and future periods.

Altogether, despite a reduced computational resolution, the results of wave model validation are generally consistent with calibration

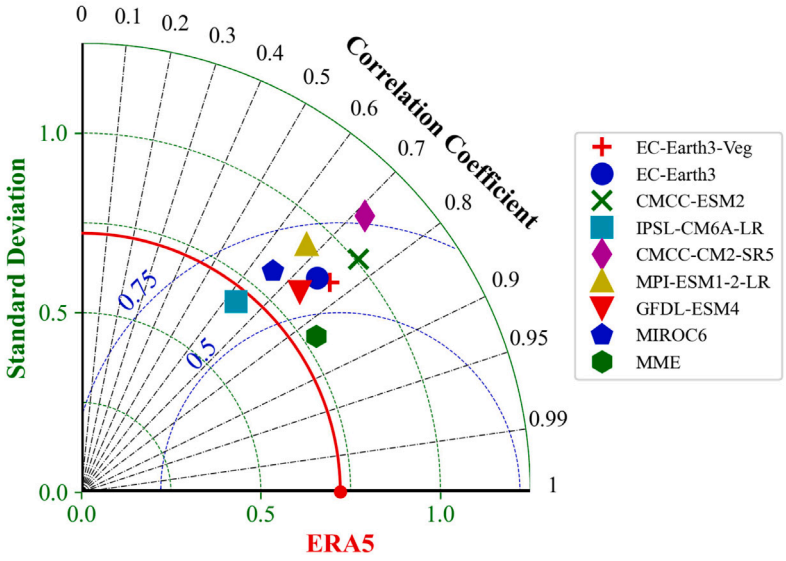

Fig. 4. Performance of single CMIP6 datasets and the MME (excludes MIROC6) for monthly WPD for the baseline period within the study area. Blue lines indicate values for CRMSE (kWm^{-2}).

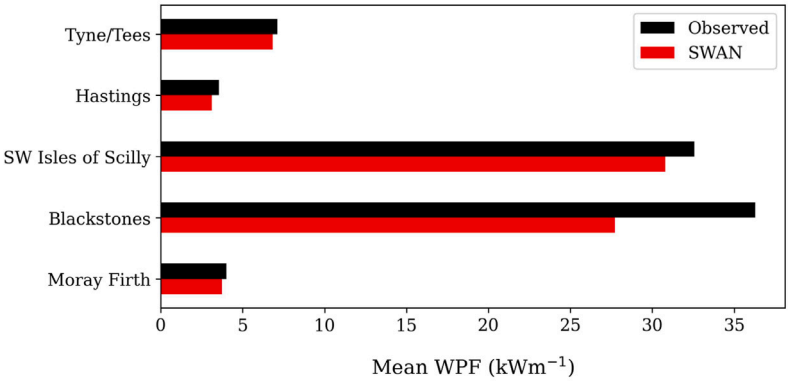

Fig. 5. Average annual observed and modelled WEF for each buoy location (2015–2024).

Table 4
Validation results for 30 min outputs of the SWAN model.

Buoy	Bias			RMSE			CC			SI		
	WEF (kWm^{-1})	H_s (m)	T_z (s)	WEF (kWm^{-1})	H_s (m)	T_z (s)	WEF	H_s	T_z	WEF	H_s	T_z
Tyne/Tees	0.71	0.10	−0.62	5.57	0.31	0.83	0.97	0.95	0.85	0.58	0.18	0.17
Hastings	−0.52	−0.07	−0.75	1.39	0.21	1.01	0.92	0.92	0.69	0.80	0.28	0.28
SW Isles of Scilly	−0.22	0.08	−1.02	4.35	0.32	1.34	0.89	0.92	0.59	0.53	0.21	0.25
Blackstones	−3.73	−0.16	−1.38	12.58	0.53	1.85	0.83	0.90	0.59	0.80	0.29	0.32
Moray Firth	1.07	0.02	−0.57	11.33	0.37	0.89	0.95	0.96	0.86	0.80	0.21	0.17

studies conducted at higher spatiotemporal resolutions [44], including subregional analyses conducted within the present study area [45]. The model is therefore sufficient to model wave energy using single CMIP6 datasets at 0.5° grid resolution.

3.3. Multi-decadal resource evolution

Multi-decadal comparison between baseline and future periods reveal generally decreasing trends in average annual WPD, increasing in severity towards the end of the century (Fig. 6(a)). The impacts are particularly pronounced in coastal regions of Northern Ireland and south-west Scotland, with decreases in average annual WPD of up to −10.8% (−56.10 Wm^{-2}) in the mid-future and −15.9% (−83.11 Wm^{-2}) for the far future relative to the historical period. Conversely, some regions of south-east England are projected to experience slight increases in average annual WPD of 0.9% (3.98 Wm^{-2}) for the mid future period, rising to 2.7% (12.39 Wm^{-2}) in the far future.

Similarly, average annual wave resources are projected to decrease throughout most of the study area (Fig. 6(b)), particularly across the North Sea, with decreases of up to −16.4% in the mid future (−688.32 Wm^{-1}) and −25.2% in the far future (−1422.73 Wm^{-1}) off the east coast of Scotland. However, negligible trends are shown in areas west of the Hebrides as well as parts of the Celtic Sea, suggesting minimal long term climate impacts on wave resources in these areas. Elsewhere, increases of up to 2.4% (440.50 Wm^{-1}) in the mid future and 4.6% (188.90 Wm^{-1}) in the far future are projected west of the Bristol Channel.

The analysis of continuous change over time, from 2015 to 2100, shows 87.8% of grid points within the study area with a statistically

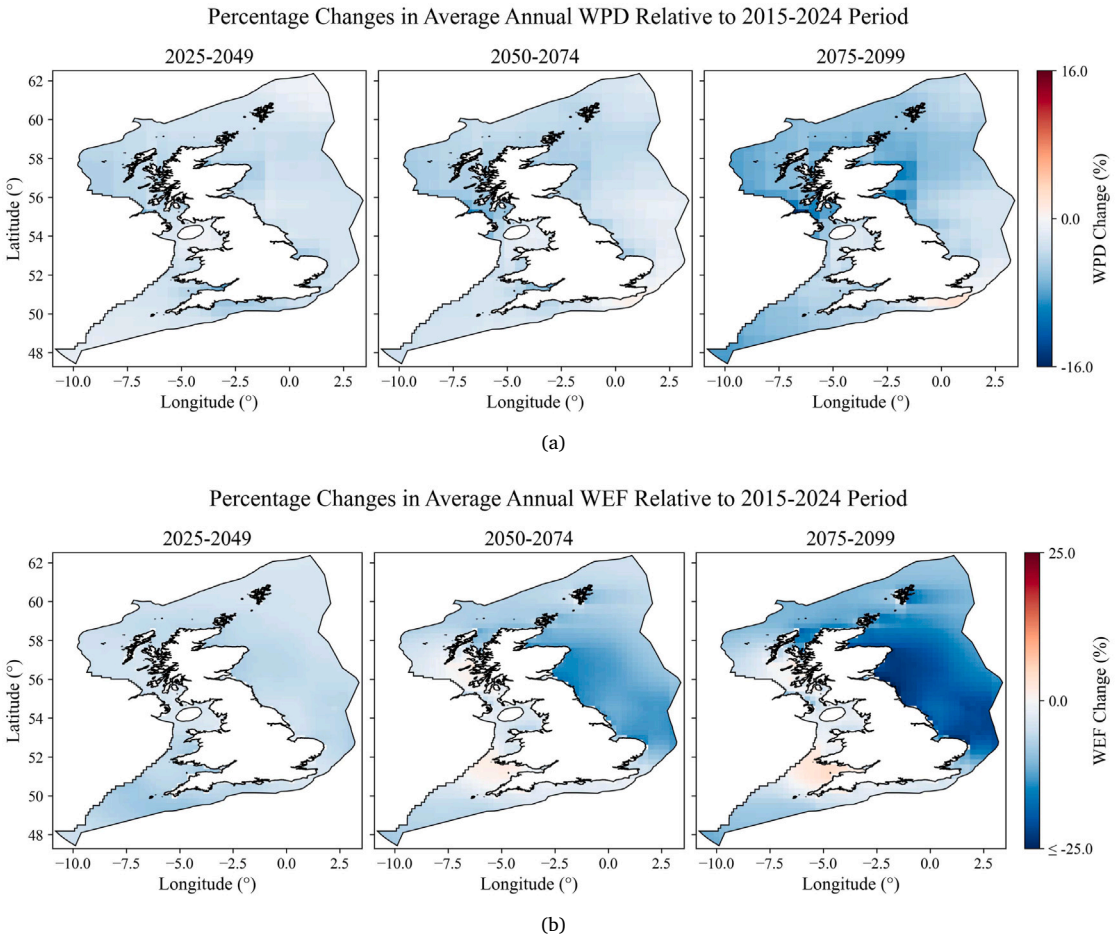

Fig. 6. Multi-decadal changes in annual average WPD (a) and WEF (b) for near future, mid future and far future relative to the baseline period.

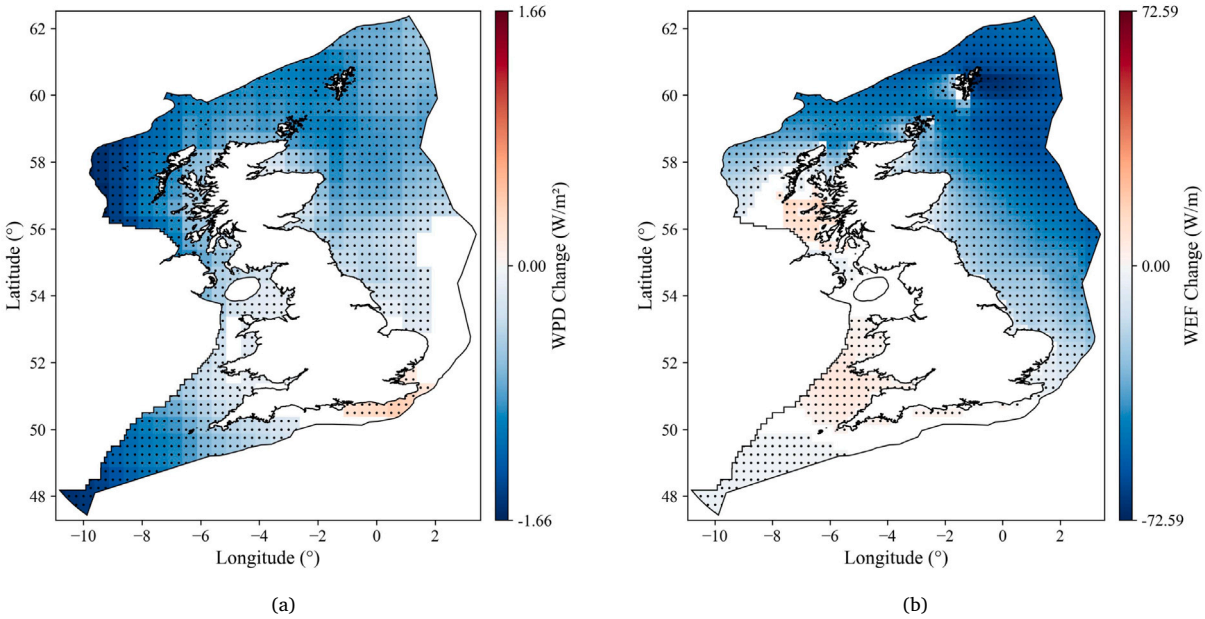

Fig. 7. Spatial distribution of regression-derived annual trends in WPD (a) and WEF (b) based on daily average values. Stippling indicates grid points with statistically significant annual trends ($p < 0.05$).

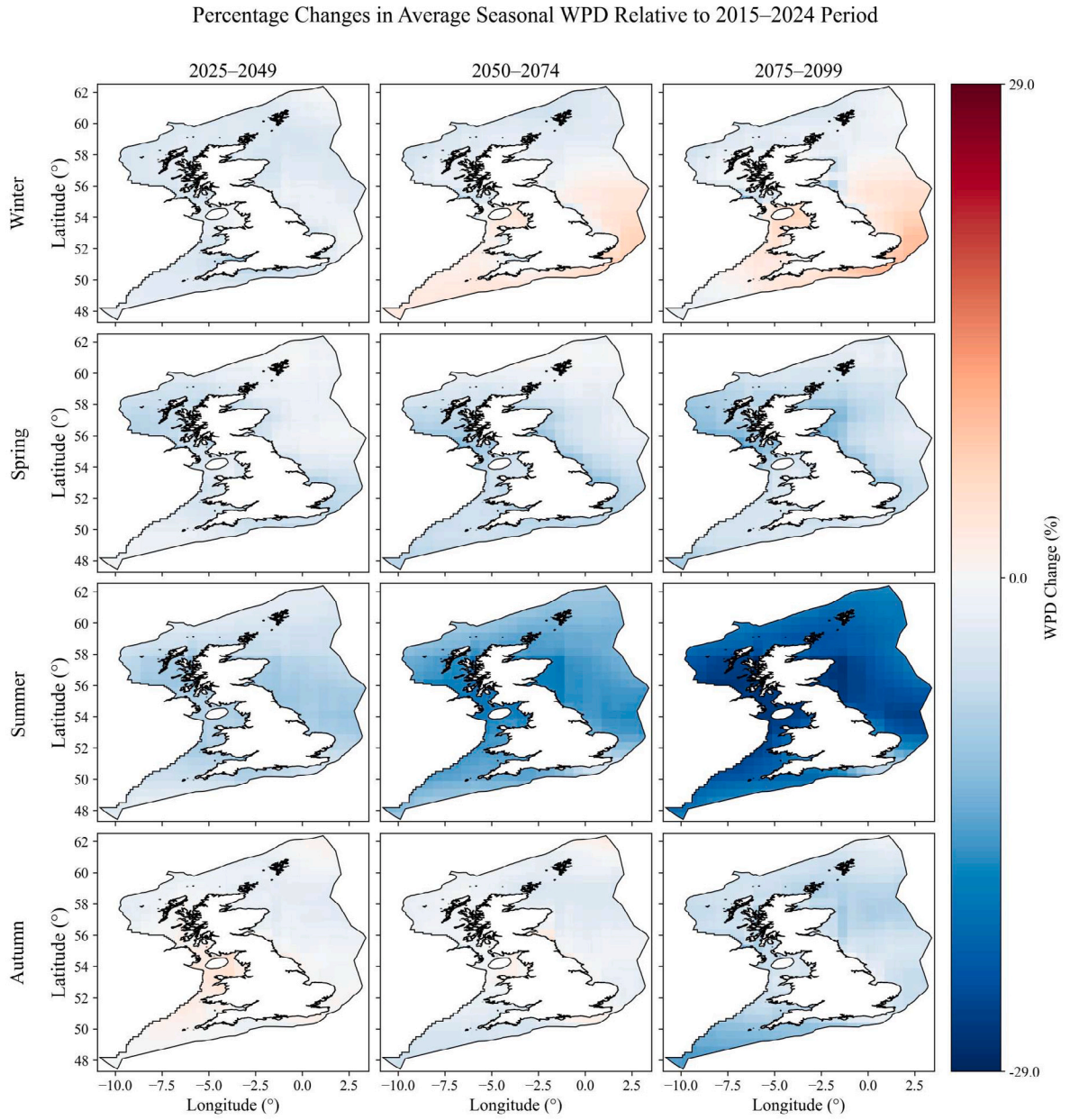

Fig. 8. Changes in seasonal WPD for near future, mid future and far future relative to the historical period.

significant trend in the wind resource per year (Fig. 7(a)). The magnitude of this trend ranges between −1.66 Wm^{-2} per year off the coast of Northern Ireland, while increases are projected in the English Channel near south-east England of up to 0.39 Wm^{-2}. Meanwhile, several regions are identified where no significant change is likely to occur, including areas of the Welsh coast and deep water areas in the North Sea. On average, the impact of climate change on wind resources was found to be −0.62 Wm^{-2} per year across the study area.

On the other hand, 85.5% of the grid points show statistically significant trends in wave resource per year, ranging in magnitude from −72.59 Wm^{-1} near Shetland to 17.25 Wm^{-1} near the Outer Hebrides, with an average of −26.01 Wm^{-1} across the study area. Meanwhile, no significant continuous change is detected for the regions in the English Channel and the Irish Sea around the Isle of Man.

From this it can be observed that the impacts of climate change on wind and wave resources vary geographically for each resource. While relatively small in magnitude, the detection of significant climate signals for each MME suggests long term shifts in resource availability with implications for the climate resilience of renewable development at these locations. That some areas, such as the west coast, experience significant decreasing trends in WPD, and negligible or opposing trends in WEF, suggests co-location with wave energy systems can potentially enhance the sustainability of offshore wind projects in the long term.

3.4. Intra-annual resource evolution

Overall decreases in annual WPD are largely driven by reductions in energy yield during summer months (June, July and August), gradually increasing in severity towards the end of the century (Fig. 8). Average seasonal WPD during these months is projected to decrease by 3.5% in the near future, 14.1% in the mid future and 21% in the far future. These findings echo those of previous wind energy assessments conducted with CMIP6 data for SSP5-8.5 reported in [22,46]. Interestingly,

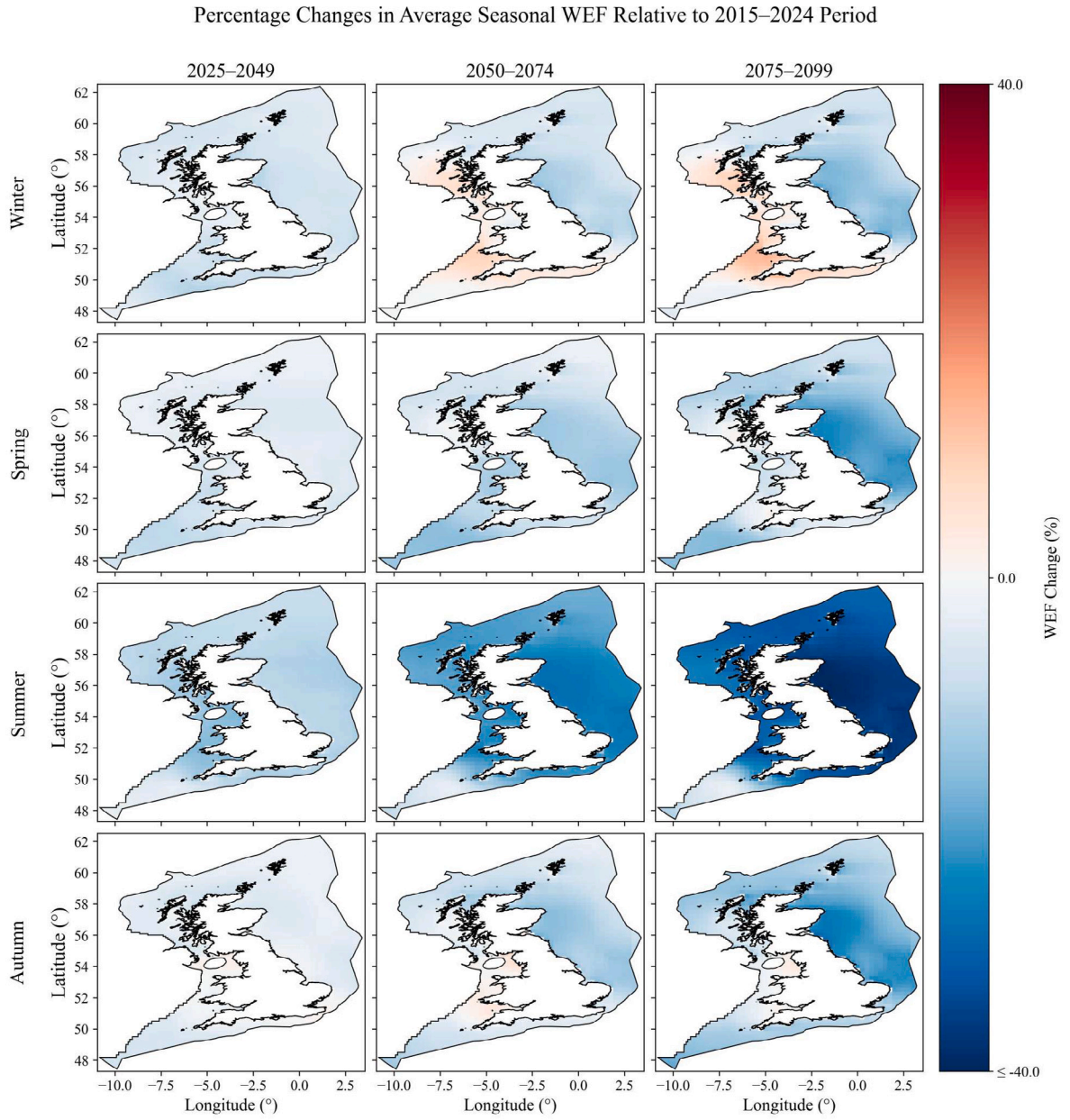

Fig. 9. Changes in seasonal WEF for near future, mid future and far future relative to the historical period.

increases are projected for winter months (December, January and February) across the southern region of the study area, with maximum increases of 0.1% (2.53 Wm^{-2}) in the near future, 7.1% (62.64 Wm^{-2}) in the mid future and 9.8% (74.39 Wm^{-2}) in the far future.

Similarly, reductions in annual wave resources are found to be driven by decreases in average resources during the summer months (Fig. 9), in particular from the mid and far future periods, by up to −28.0% (−718.60 W/m) and −40.4% (−518.02 W/m), respectively. On the other hand, increases in average wave resources for winter months are also detected across much of the west coast of the UK, of up to 9.3% (1142.68 W/m) in the mid future and 13.5% (1228.94 W/m) in the far future. Previous research suggests this may be caused by the projected poleward displacement of storm tracks for higher latitudes, leading to year-round reductions in available wind and wave resources [47].

That WPD and WEF exhibit similar reductions in energy potential during summer suggests co-located wind-wave may remain vulnerable to decreasing levels of generation during summer months throughout the 21st century. However, positive trends in both resources are exhibited in shared locations for winter, particularly for areas in the Celtic Sea and the English Channel, suggesting climate change may act to enhance resource synergies during these months.

3.5. Evolution of resource stability

Analysis of wind resource stability shows gradually increasing trends for CoV from the mid future period onward, following slight decreasing trends in the near future across much of the study area (Fig. 10(a)). Maximum increases of 3.6%, 9.6% and 15.0% for near, mid and far future periods, respectively, are projected in the North Sea east of Norwich, with more modest trends projected in northwestern regions of the study area. This aligns with previous research that found similar magnitudes of changes in CoV in the North Sea, and that these changes are unique to high emission scenarios [22]. Overall, grid averaged changes in CoV are projected with increases of 4.1% in the mid-future and 8.4% for the far future.

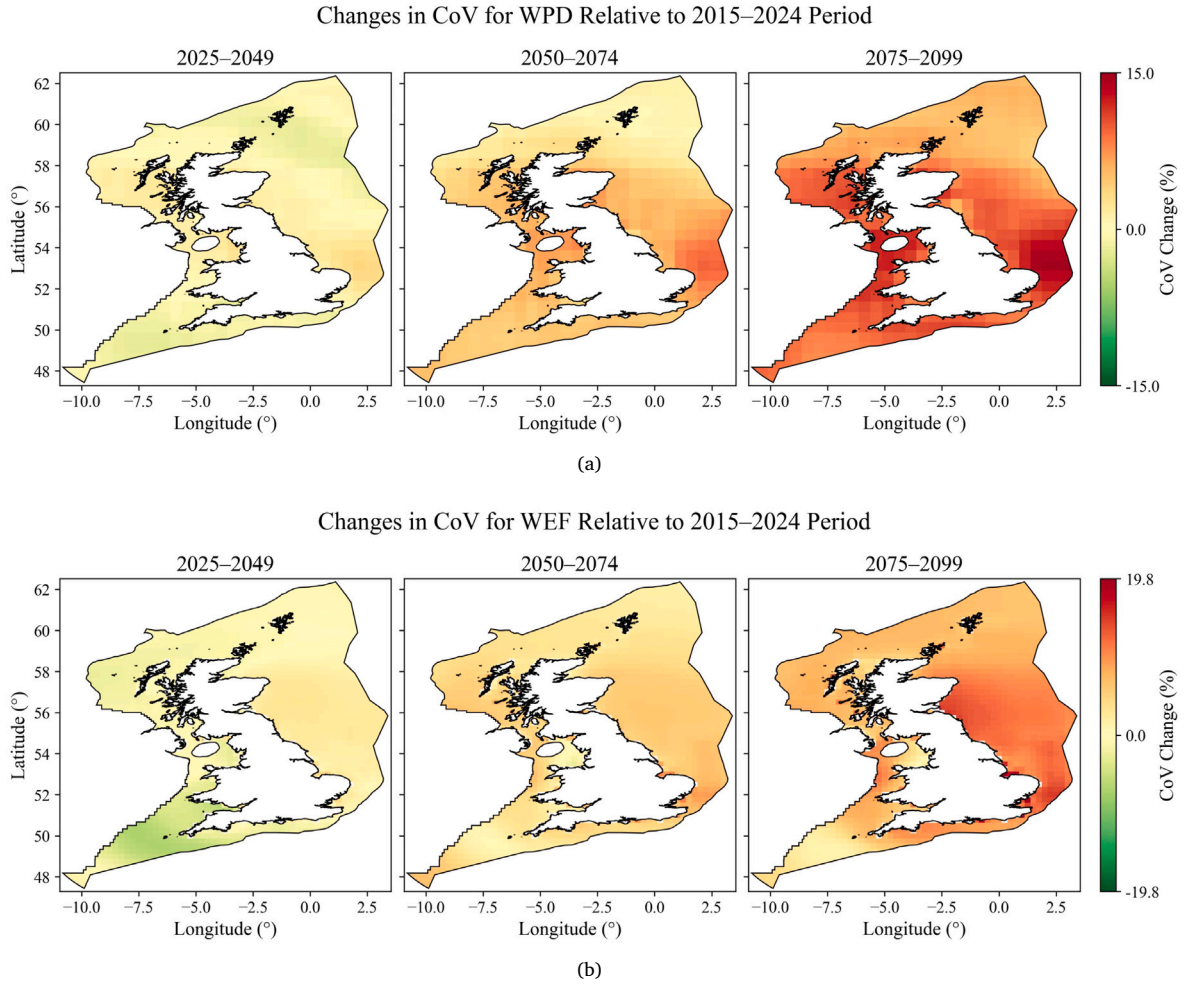

Fig. 10. Multi-decadal changes in CoV for WPD (a) and WEF (b) for near future, mid future and far future relative to the historical period.

The wave resource shows similar trends for CoV, with initial decreases of up to −7.2% in the near future in the Celtic Sea (Fig. 10(b)). However, increases of up to 4.7%, 10.6% and 19.8% for near, mid and far future periods, respectively, are shown for coastal regions of south-east England, implying particularly localised climate impacts on wave resource stability, amidst grid averaged increases of 4.1% and 8.0% in CoV for the mid and far future periods, respectively. Nevertheless, it remains unclear whether co-location may effectively combat this destabilisation due to the theoretical assessment of resource availability in the present study.

4. Summary & conclusions

This study quantifies long-term climate change impacts on marine wind–wave resources in the UK for the remainder of the 21st century under a high emission climate change scenario. This was achieved through the construction of two MMEs for wind and wave energy, respectively, derived from seven available CMIP6 datasets for the SSP5-8.5 scenario. The SWAN wave model was implemented for each dataset to provide a robust assessment of the evolution of renewable wave energy from 2015 to 2100. As the analysis is conducted under the SSP5-8.5 scenario, the results presented here are specific to this high-emission pathway and therefore represent potential upper-bound climate change impacts on marine wind–wave resources. The key research findings of the present study are summarised as follows.

Several CMIP6 models, namely the EC-Earth3 and EC-Earth3-Veg datasets, were found to outperform others in terms of their ability to emulate near-surface wind speeds across northwestern Europe. Moreover, the use of MMEs for assessing energy potential demonstrates superiority over the use of single models, characterised by reduced bias and higher correlation with the reanalysis data. In addition, the wave model calibration determined ST6 as the optimal third generation mode for the purposes of modelling wave energy with ERA5 in the study area. The most important parameters adjusted to improve accuracy were identified as the terms for cumulative and local dissipation, and the associated windscaling value.

Under a high emission scenario, climate change is likely to result in gradual reductions in energy potential for both wind and wave resources. Although comparable amounts of area exhibit significant annual change for each resource (87.8% to 85.5% of the study area), their spatial trends often diverge. As such, decreases in wind energy occur in regions where wave impacts are minimal, and vice versa. This suggests that future offshore wind developments along the west coast of the UK may be less vulnerable to climate-driven reductions in energy potential if integrated with co-located wave energy systems. However, reductions are primarily driven by decreases in energy potential during the summer months for both wind and wave resources. Conversely, opposing spatial trends for winter months are shown, with gradual increases in average wave power across the west coast of the UK, and increases in wind power across the southern half of the EEZ. This requires further investigation with respect to seasonal climate

extremes and practical energy yields, and presents opportunities for future works. In terms of stability, both resources are projected to experience temporary decreases in variability in the near future, followed by gradual increases in the mid and far future. These findings indicate that increasing variability in marine energy resources should be considered in future offshore energy planning, and warrants further study into the potential role of hybrid wind–wave systems in maintaining more stable generation profiles under climate change.

The limitations of the present study are largely underpinned by the ability of the wave model to simulate realistic ocean conditions relevant for energy capture. The underestimation of modelled WEF at Blackstones, in particular, highlights the difficulties in wave model calibration for larger domains with complex sea states. Although the model is shown to perform well overall, the analysis does not account for these underestimations in areas dominated by Atlantic swell. On the other hand, the spatial resolution of nested SWAN outputs presents challenges for the accurate assessment of energy potential for inshore regions and complex coastlines that characterise much of the west coast of Scotland. The deployment of SWAN on smaller scales nearshore is therefore encouraged for a more accurate assessment of localised climate change impacts on wave resources.

A second limitation is tied to the relatively coarse spatiotemporal resolution of the CMIP6 data. This may also result in underestimations of renewable resources largely driven by the inability to reflect extreme values. In the present study, this is compounded by the use of the MME, which cancels out extreme highs and lows in addition to single model bias. As a result, the data used here is unsuitable for an assessment of the impacts of climate change on practical energy yields, as well as energy droughts and the occurrence of storms, and provides an important avenue for subsequent investigation.

CRediT authorship contribution statement

John-Luke McWhirter: Writing – original draft, Software, Methodology, Formal analysis, Conceptualization. **Bahareh Kamranzad:** Writing – review & editing, Supervision, Methodology, Conceptualization. **George Lavidas:** Writing – review & editing, Supervision, Methodology. **Gil Lemos:** Writing – review & editing, Methodology.

Declaration of competing interest

The authors declare that they have no known competing financial interests or personal relationships that could have appeared to influence the work reported in this paper.

Acknowledgements

The research has received from the Engineering and Physical Sciences Research Council (EPSRC), United Kingdom under the project *Hybrid Ocean Renewables in a Changing Climate*. The primary author gratefully acknowledges Dr Ourania Altiparmaki for providing access to literature and for helpful discussions.

Data availability

Data will be made available on request.

References

[1] IPCC, Climate Change 2021: The Physical Science Basis, Cambridge University Press, Cambridge, 2021, Contribution of Working Group I to the Sixth Assessment Report of the Intergovernmental Panel on Climate Change.
[2] United Nations, Causes and effects of climate change, 2025, Available at: https://www.un.org/en/climatechange/science/causes-effects-climate-change. (Accessed 22 July 2025).
[3] H. Ritchie, 4 charts explain greenhouse gas emissions by countries and sectors, 2024, World Resources Institute. Available at: https://www.wri.org/insights/4-charts-explain-greenhouse-gas-emissions-countries-and-sectors. (Accessed 24 July 2025).
[4] I.E. Agency, Offshore Wind Outlook 2019, Technical Report, International Energy Agency, 2019, URL https://www.iea.org/reports/offshore-wind-outlook-2019.
[5] E. Dallavalle, M. Cipolletta, V.C. Moreno, V. Cozzani, B. Zanuttigh, Towards green transition of touristic islands through hybrid renewable energy systems. a case study in Tenerife, Canary islands, Renew. Energy 174 (2021) 426–443.
[6] UN Atlas of the Oceans, Facts, 2025, Available at: https://www.oceansatlas.org/facts/en/. (Accessed 20 October 2025).
[7] Department for Energy Security and Net Zero, Clean Power 2030 Action Plan: a New Era of Clean Electricity, Technical Report, UK Government, 2024, URL https://assets.publishing.service.gov.uk/media/677bc80399c93b7286a396d6/clean-power-2030-action-plan-main-report.pdf.
[8] Wave Energy Scotland, UK government launches marine energy taskforce to accelerate wave and tidal innovation, 2025, Available at: https://www.waveenergyscotland.co.uk/news/2025/june/uk-government-launches-marine-energy-taskforce-to-accelerate-wave-and-tidal-innovation/. (Accessed 20 October 2025).
[9] T. Chen, M. Wang, R. Babaei, M. Safa, A. Shojaei, Technoeconomic analysis and optimization of hybrid solar-wind-hydrodiesel renewable energy systems using two dispatch strategies, Int. J. Photoenergy (2023) 1–20.
[10] X. Chen, H. Mao, N. Cheng, L. Ma, Z. Tian, Y. Luo, C. Zhou, H. Li, Q. Wang, W. Kong, J. Fan, Climate change impacts on global photovoltaic variability, Appl. Energy 374 (2024) 1–17.
[11] S. Astariz, G. Iglesias, Output power smoothing and reduced downtime period by combined wind and wave energy farms', Energy 97 (2016) 69–81.
[12] S. Astariz, G. Iglesias, Enhancing wave energy competitiveness through co-located wind and wave energy farms. a review on the shadow effect, Energies 8 (7) (2015) 7344–7366.
[13] C. Weiss, R. Guanche, B. Ondiviela, O. Castellanos, J. Juanes, Marine renewable energy potential: A global perspective for offshore wind and wave exploitation, Energy Convers. Manage. 177 (2018) 43–54.
[14] International Energy Agency, World Energy Outlook 2024, Technical Report, International Energy Agency, 2024, URL https://iea.blob.core.windows.net/assets/140a0470-5b90-4922-a0e9-838b3ac6918c/WorldEnergyOutlook2024.pdf.
[15] C. Kalogeri, G. Galanis, C. Spyrou, D. Diamantis, F. Baladima, M. Koukoula, G. Kallos, Assessing the European offshore wind and wave energy resource for combined exploitation, Renew. Energy 101 (2017) 244–264.
[16] F. Ferrari, G. Besio, F. Cassola, A. Mazzino, Optimized wind and wave energy resource assessment and offshore exploitability in the mediterranean sea, Energy 190 (2020) 1–15.
[17] A. Majidi, V. Ramos, T. Calheiros-Cabral, P. Santos, L. Neves, F. Taveira-Pinto, Integrated assessment of offshore wind and wave power resources in mainland Portugal, Energy 308 (2024) 1–13.
[18] S. Gallagher, R. Tiron, E. Whelan, E. Gleeson, F. Dias, R. McGrath, The nearshore wind and wave energy potential of Ireland: A high resolution assessment of availability and accessibility, Renew. Energy 88 (2016) 494–516.
[19] A. Azzellino, C. Lanfredi, L. Riefolo, V. Santis, P. Contestabile, D. Vicinanza, Combined exploitation of offshore wind and wave energy in the Italian seas: A spatial planning approach, Front. Energy Res. 7 (2019) 1–15.
[20] S. Astariz, G. Iglesias, Selecting optimum locations for co-located wave and wind energy farms. part II: A case study, Energy Convers. Manage. 122 (2016) 599–608.
[21] A. Martinez, G. Iglesias, Wind resource evolution in europe under different scenarios of climate change characterised by the novel shared socioeconomic pathways, Energy Convers. Manage. 234 (2021) 1–16.
[22] A. Martinez, L. Murphy, G. Iglesias, Evolution of offshore wind resources in northern Europe under climate change, Energy 269 (2023) 1–11.
[23] A. Ribeiro, M. deCastro, X. Costoya, L. Rusu, J. Dias, M. Gomez-Gesteira, A delphi method to classify wave energy resource for the 21st century: Application to the NW Iberian Peninsula, Energy (2021) 1–14.
[24] M. deCastro, G. Lavidas, B. Arguile-Perez, P. Carracedo, N. deCastro, X. Costoya, M. Gomez-Gesteira, Evaluating the economic viability of near-future wave energy development along the galician coast using LCoE analysis for multiple wave energy devices, J. Clean. Prod. 463 (2024) 1–17.
[25] R. Vázquez, C. Gutiérrez, P. de León, J. Nieto-Borge, D. Sein, W. Cabos, Climate change impact in offshore energy resources along the Spanish coasts based on a high-resolution regionally coupled model, Renew. Energy 249 (2025) 1–11.

[26] K. Riahi, D. Vuuren, E. Kriegler, J. Edmonds, B. O'Neill, S. Fujimori, N. Bauer, K. Calvin, R. Dellink, O. Fricko, W. Lutz, A. Popp, J. Crespo Cuaresma, S. KC, M. Leimbach, L. Jiang, T. Kram, S. Rao, J. Emmerling, K. Ebi, T. Hasegawa, P. Havlik, F. Humpenöder, L. Silva, S. Smith, E. Stehfest, V. Bosetti, J. Eom, D. Gernaat, T. Masui, J. Rogelj, J. Strefler, L. Drouet, V. Krey, G. Luderer, M. Harmsen, K. Takahashi, L. Baumstark, J. Doelman, M. Kainuma, Z. Klimont, G. Marangoni, H. Lotze-Campen, M. Obersteiner, A. Tabeau, M. Tavoni, The shared socioeconomic pathways and their energy, land use, and greenhouse gas emissions implications: An overview, Glob. Environ. Chang. 42 (2017) 153–168.

[27] P. Li, J. Lian, C. Ma, J. Zhang, Complementarity and development potential assessment of offshore wind and solar resources in China seas, Energy Convers. Manage. 296 (2023) 1–15.

[28] H. Zhao, P. Chen, W. Zhang, S. Yan, J. Yang, J. Kong, On the capability of SWAN model for south atlantic ocean wave simulation, Ocean. Dyn. 75 (51) (2025) 1–17.

[29] M. Alday, F. Ardhuin, G. Dodet, M. Accensi, Accuracy of numerical wave model results: application to the atlantic coasts of Europe, Ocean. Sci. 18 (2022) 1665–1689.

[30] Centre for Environment, Fisheries and Aquaculture Science, QA/QC procedure, 2025, Available at: https://www.cefas.co.uk/data-and-publications/wavenet/qa-qc-procedure/. (Accessed 21 October 2025).

[31] D. Satymov, D. Bogdanov, M. Dadashi, G. Lavidas, C. Breyer, Techno-economic assessment of global and regional wave energy resource potentials and profiles in hourly resolution, Appl. Energy 364 (2024) 1–18.

[32] P. Jones, First- and second-order conservative remapping schemes for grids in spherical coordinates, Mon. Weather Rev. 127 (1999) 2204–2210.

[33] Z. Shu, Q. Li, P. Chan, Investigation of offshore wind energy potential in Hong Kong based on Weibull distribution function, Appl. Energy 156 (2015) 362–373.

[34] R. Ris, L. Holthuijsen, N. Booij, A third-generation wave model for coastal regions, J. Geophys. Res. 104 (C4) (1999) 7667–7681.

[35] G. Lavidas, V. Venugopal, Application of numerical wave models at European coastlines: A review, Renew. Sustain. Energy Rev. 92 (2018) 489–500.

[36] H. Van der Zant, A. Pillet, A. Schaap, S. Stark, T. de Weijer, A. Cahyaningwidi, B. Lehner, The energy park of the future: Modelling the combination of wave-, wind- and solar energy in offshore multi-source parks, Heliyon 10 (5) (2024) 1–14.

[37] C. Tebaldi, R. Knutti, The use of the multi-model ensemble in probabilistic climate projections, Phil. Trans. R. Soc. A 365 (2007) 2053–2075.

[38] J. Xu, J. Li, S. Pan, Y. Yao, L. Chen, Z. Wu, Assessment of wind and wave energy in China seas under climate change based on CMIP6 climate model, Energy 310 (2024) 1–20.

[39] F. Birol, F. Bignalet-Cazalet, M. Cancet, J.-A. Daguze, W. Fkaier, E. Fouchet, F. Léger, C. Maraldi, F. Niño, M.-I. Pujol, N. Tran, Understanding uncertainties in the satellite altimeter measurement of coastal sea level: insights from a round-robin analysis, Ocean. Sci. 21 (1) (2025) 133–150.

[40] D. Carvalho, A. Rocha, M. Gómez-Gesteira, C. Silva Santos, WRF wind simulation and wind energy production estimates forced by different reanalyses: Comparison with observed data for Portugal, Appl. Energy 117 (2014) 116–126.

[41] W. Rogers, A. Bananin, D. Wang, Observation-consistent input and whitecapping dissipation in a model for wind-generated surface waves: Description and simple calculations, J. Atmos. Ocean. Technol. 29 (2012) 1329–1346.

[42] P. Hwang, H. García-Nava, F. Ocampo-Torres, Observations of wind wave development in mixed seas and unsteady wind forcing, J. Phys. Oceanogr. 41 (12) (2011) 2343–2362.

[43] W. Zhang, H. Zhao, G. Chen, J. Yang, Assessing the performance of SWAN model for wave simulations in the bay of Bengal, Ocean Eng. 285 (2023) 1–23.

[44] Y. Lin, S. Dong, Z. Wang, C. Guedes Soares, Wave energy assessment in the China adjacent seas on the basis of a 20-year SWAN simulation with unstructured grids, Renew. Energy 136 (2019) 275–295.

[45] S. Neill, Wave resource characterization and co-location with offshore wind in the Irish Sea, Renew. Energy 222 (2024) 1–13.

[46] A. Hahmann, O. García-Santiago, A. Peña, Current and future wind energy resources in the north sea according to CMIP6, Wind. Energy Sci. 7 (6) (2022) 2372–2391.

[47] G. Lemos, M. Menendez, A. Semedo, P. Miranda, M. Hemer, On the decreases in north atlantic significant wave heights from climate projections, Clim. Dyn. 57 (2021) 2301–2324.